

Custom Molecular Design of Ligands for Perovskite Photovoltaics

Meifang Yang, Tian Tian, Wenhui Feng, Lianzhou Wang,* and Wu-Qiang Wu*



Cite This: *Acc. Mater. Res.* 2021, 2, 1141–1155



Read Online

ACCESS |



Metrics & More



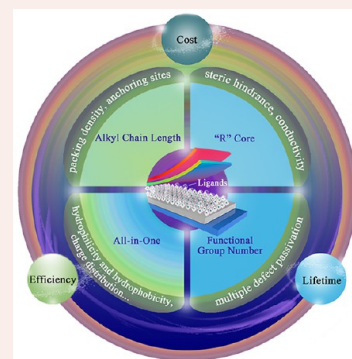
Article Recommendations



Supporting Information

CONSPECTUS: Perovskite photovoltaics have witnessed overwhelming success owing to their high power conversion efficiency, low voltage deficit, sensitive photoelectric response and good operational stability. However, solution-processed, polycrystalline perovskite films inevitably contain a high density of crystallographic defects, such as uncoordinated ions and dangling bonds at the surfaces and grain boundaries, which can result in charge recombination, thus causing energy loss and impaired device performance. These intrinsic imperfections can be remedied through a chemically induced intermarriage between halide perovskites of soft crystallographic nature and judiciously designed exotic ligand molecules. Utilizing rational molecular design of the component moieties, i.e., the core and tail functional groups, the ligand molecules can be endowed with both more comprehensive and salient advantages to further boost device performance, thus setting perovskite photovoltaics on course for a more prosperous future.

In this Account, we present our narrative of designing a series of favorable ligand molecules with multifunctionalities in terms of crystal growth modulation, grains cross-linking, defect passivation, surface functionalization, phase stabilization, and moisture invasion inhibition of perovskite films and summarize the advances made in designing molecular level custom ligands that have progressively lifted the record performances of perovskite photovoltaics. We first identify the origins of imperfections in perovskites and their detrimental impacts on device efficiency and stability. We then review feasible rules for ligand design, including tuning the length of the linear or branched alkyl chain core, the substitution of one or more carbon atoms with O, P, S, or NH, and the number of functional groups (double, triple, quadruple, or even multiple ones), to design “all-in-one” ligands with ideal molecular structures and multifunctionalities. The chemical interactions between ligands and perovskites (e.g., coordination bond, ionic bond, hydrogen bond, electrostatic interaction and chelation, etc.) are discussed, aiming to elucidate their impact on the necessary trade-off between defect passivation efficacy and charge transport property in ligand-modified perovskite films, and establish a triangular structure–property–performance relationship for perovskite-based optoelectronic devices with ligands modulation and passivation. We also insightfully explore novel ligand management strategies in perovskite quantum dots, especially the development of ligand-assisted cation exchange and surface ligand density optimization. Finally, we present an astute perspective of future trends in the rational design of innovative ligand molecules with desired structures and properties for more efficient, stable, perovskite-based optoelectronic devices.



1. INTRODUCTION

Over the past decade, the emerging perovskite photovoltaics (PVs) have attracted great research interest. The certified efficiency of perovskite solar cells (PSCs) has reached 25.5%, which is already on par with or even outperforming other thin film PV technologies.^{1–5} In addition to the high efficiencies, perovskite PVs witnessed astonishing success in other aspects, such as the lowest voltage deficit of 0.30 V (less than crystalline silicon solar cells, 0.38 V), very sensitive photoelectric response at weak light condition (i.e., >40% efficiency for indoor PV application), and good operational stability that passed the industrial IEC 61215:2016 Damp Heat and Humidity Freeze tests.^{6–8} The above-mentioned achievements are mainly attributed to the value-added intermarriage between halide perovskites of soft crystallographic natures and exotic ligands with ingenious molecular structures.

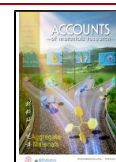
Owing to the ionic nature of perovskite semiconductors, solution-processed polycrystalline perovskite films inevitably

contain a high density of crystallographic defects, such as uncoordinated ions and dangling bonds at the surfaces and grain boundaries (GBs), which incur charge recombination and limit further performance enhancement (Supporting Information Note 1).^{9–11} Moreover, notorious issues including the volatility of the organic cations, migration of charged ions and/or moisture sensitivity impose great challenges to further improve the life-span of perovskite PVs.^{12,13} Fortunately, the intrinsic imperfections can be remedied, while the inherent stability puzzle can be facily tackled through robust ligands modulation and passivation. It is the molecular design of the

Received: May 13, 2021

Revised: September 13, 2021

Published: October 6, 2021



ACS Publications

© 2021 Accounts of Materials Research.
Co-published by ShanghaiTech
University and American Chemical
Society. All rights reserved.

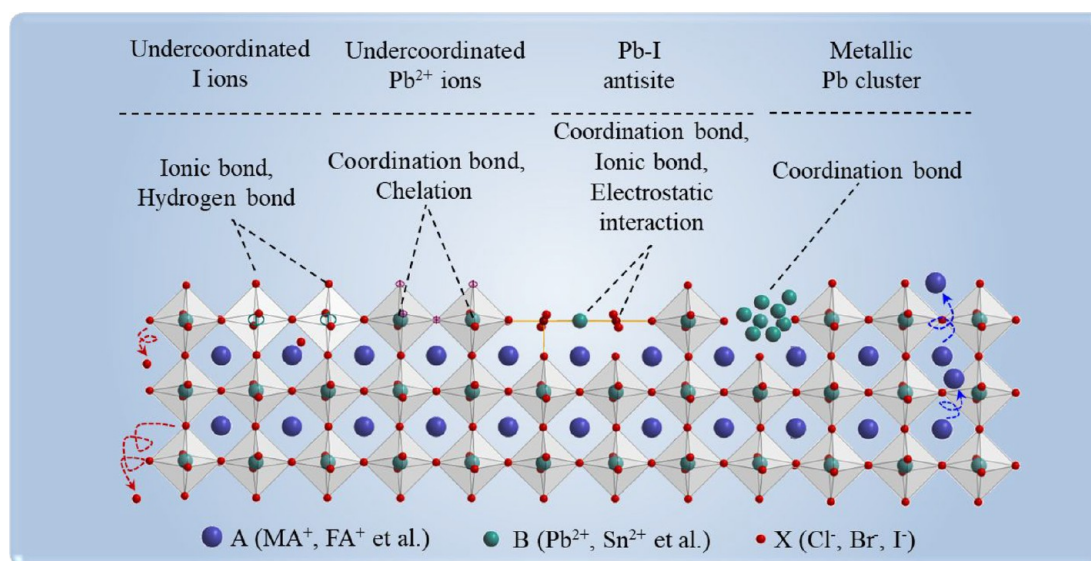


Figure 1. Imperfections in perovskite film and their passivation by coordination bond, ionic bond, hydrogen bond, electrostatic interaction, and chelation. The mobile halide ions and mobile organic cations are denoted by red arrow and blue arrow, respectively.

ligands, namely, the organic moieties of the core and the functional tail groups, which plays critical roles in simultaneously improving the efficiency and stability of PSCs, thus bringing prosperity for perovskite PVs.

To date, there are several hundred ligand molecules reported used in PSCs, but the selection of these molecules seems to be either random or dictated by their commercial availability.^{14–16} No clear rationale has been established to guide the molecular design of effective ligand molecules that can best stimulate the potential of perovskite materials, and so continuously lift the record performance of perovskite PVs. In this regard, purposely designed ligands are keys to the practical application of high-performance PSCs, yet the concept of “molecular design” has not drawn much attention in the field.

In this Account, we elucidate the triangular molecular structure-optoelectronic property-device performance relationship and outline how the custom design of ligands on a molecular level can further advance the device performance of perovskite PVs. Starting from the most simple ligand (i.e., the primary amine with a structure of R-NH₂), we discuss recent advances in tailoring the molecular structures of ligands, such as modifying the linear or branched alkyl chain core, modulating functional groups with N-, O-, S-, or P-donors, and tuning the numbers of functional groups. With full consideration of the chemical interaction type and strength between perovskites and ligands, we present ideal “all-in-one” multidentate ligands with multifunctionalities in terms of crystal growth modulation, defect passivation, surface functionalization, phase stabilization, and the inhibition of moisture invasion. Together, these functionalities can tap the omnibearing potential of perovskite materials and devices. Finally, we provide guidance about novel ligand molecules design for more efficient, stable perovskite-based optoelectronic devices and offer our perspectives on the future development of this promising field.

2. MOLECULAR DESIGN OF LIGANDS

To date, various representative molecules and/or ligands have been designed and employed to remedy the imperfections of perovskites. These smartly designed ligands strongly interact

with perovskites through coordination bonds, ionic bonds, hydrogen bonds, electrostatic interaction, and chelation (Figure 1). Obviously, suppressing the defect formation and reducing the number of defects are prerequisites to attaining the best performance of perovskite PVs, ideally breaking through the Shockley–Queisser (SQ) limit.^{17–22} The passivation of specific types of defects is influenced by the molecular structure of the ligand; passivation efficacy can guide molecular design to evolve more ideal ligands.^{23–26} In this section, we mainly summarize the efforts made by our team and other researchers in rationally tailoring the molecular structures of a variety of ligands (i.e., amines, amino acids, zwitterions, surfactants, and other multidentate ligands) for efficient and stable PSCs (Supporting Information Note 2).^{27–29}

Specifically, we will focus on tailoring the molecular structures (e.g., alkyl chain length, the constitution of organic moiety R core and/or the number of functional groups, etc.) of ligands, exploring their multifunctionalities (e.g., defect passivation, crystal growth modulation, interfacial carrier dynamics optimization, and surface protection and functionalization, as well as phase stabilization of the perovskite films, etc.), and highlighting their omnibearing potentials to markedly improve the efficiency and stability of perovskite PVs. We provide a roadmap of progressively designing more advanced “all-in-one” multidentate ligands that can perfectly heal the imperfections of perovskites.

2.1. Regulation of Alkyl Chain Length

The length of the linear alkyl chain core can determine the anchoring sites of amine ligands on perovskites, which is crucial in modulating the crystal growth, interfacial carrier transport, and defect passivation efficacy of perovskite films and devices. Recently, a versatile concept of “primary amine passivation” with molecules of “R-NH₂” or “NH₂-R-NH₂” strongly bonding on various perovskite compositions was introduced for constructing efficient and stable PSCs.³⁰ On one hand, the amines could universally passivate the surface crystallographic defects and/or A-site vacancies through strong chemical interaction between perovskite and -NH₂ tails. On the other hand, the surface anchoring of amine ligands enabled

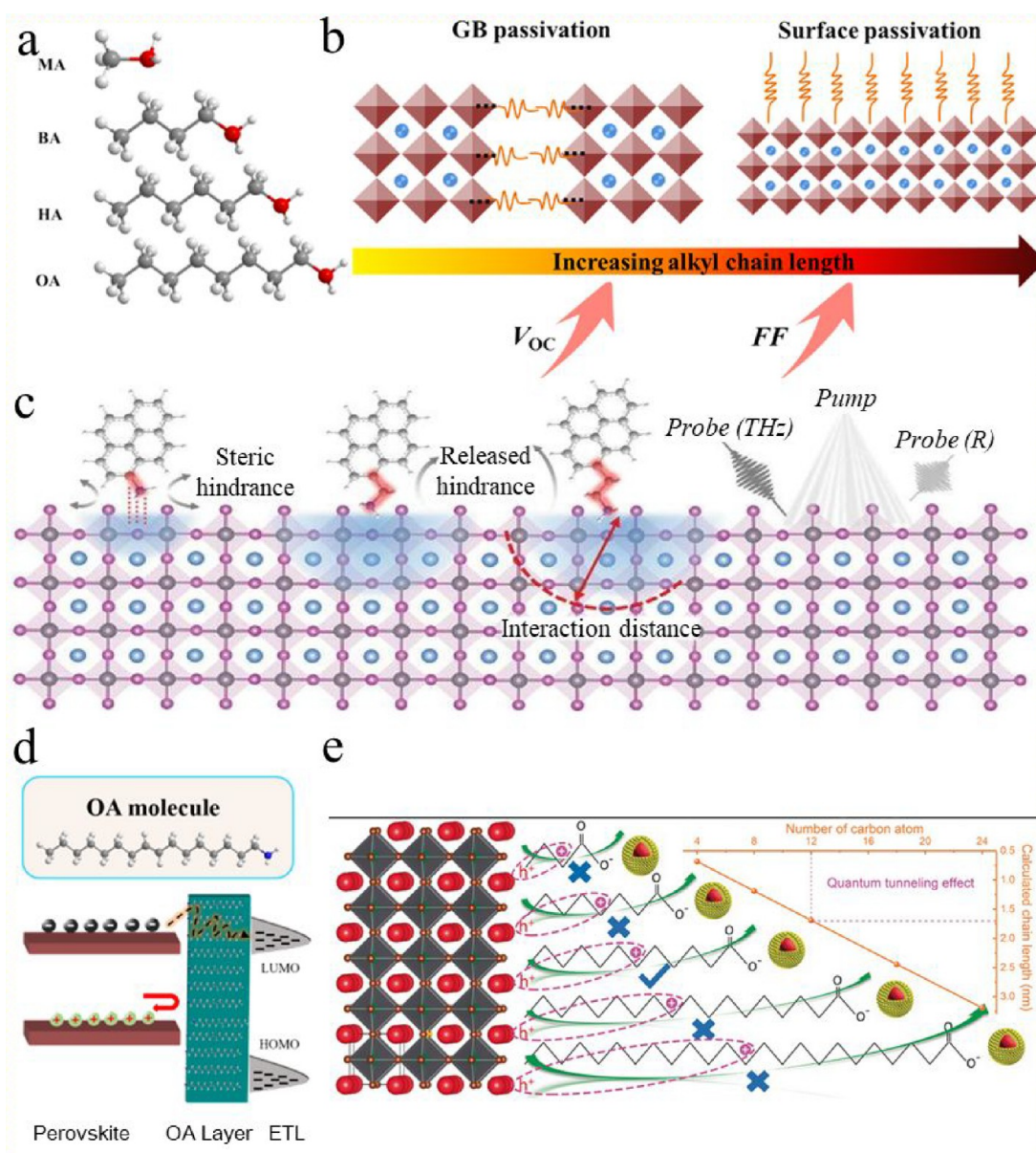


Figure 2. (a) Chemical structures of UAA molecules. (b) The relationship between alkyl chain length of UAAs and defect passivation efficacy. (c) The influence of intercalation configuration and the interaction distance revealed by the combination of transient reflection spectroscopy and time-resolved terahertz spectroscopy. (d) The OAm layer serving as a tunneling contact between the perovskite layer and ETL. (e) The interaction between CsPbBr₃ film and CuInS₂/ZnS QDs with different alkyl chain lengths. (a, b) Reproduced with permission from ref 30. Copyright 2020 Royal Society of Chemistry. (c) Reproduced with permission from ref 3. Copyright 2021 American Association for the Advancement of Science. (d) Reproduced with permission from ref 12. Copyright 2020 Elsevier. (e) Reproduced with permission from ref 31. Copyright 2020 Wiley.

exposure of the hydrophobic core chain, which functionalized the perovskite film surface with improved optoelectronic properties and stability. Starting from the simplest primary amines with a structure of "R-NH₂", we correlated the alkyl chain length (varying from one carbon to eight carbons) of unilateral alkylamine (UAA) molecules, namely, methylamine (MA), *n*-butylamine (BA), hexylamine (HA), and octylamine (OA), to the defect passivation efficacy on the surface and/or at GBs of perovskite films (Figure 2a and 2b). Interestingly, short-chain amines with alkyl chains of less than six carbons tended to anchor surrounding GBs and so passivate shallow defects, while some portion of long-chain amines of six or more carbons preferred to be spontaneously repelled to the film surface, thus capable of passivating both the shallower traps at GBs and the deep-level defects on the film surface. The PSC

modified with OA achieved a champion power conversion efficiency (PCE) of 21.5%, accompanied by a V_{oc} of 1.16 V, which corresponded to a low V_{oc} deficit of 0.35 V.³⁰ Yang et al. modulated the different lengths of alkyl chain in conjugated pyrenes containing ammonium groups, 2-(pyren-1-yl)ethan-1-aminium iodide and found that organic ammonium cations with longer alkyl chains bind well with the inorganic moieties in perovskites, which released the steric hindrance and significantly increased the interaction distance between the conjugated ligands and perovskites lattice (Figure 2c). The 2-(pyren-1-yl)ethan-1-aminium iodide (PREA) enhanced hole mobility and elevated the PCEs up to 23.0%, relative to that of a reference perovskite, and improved the device operational stability.³

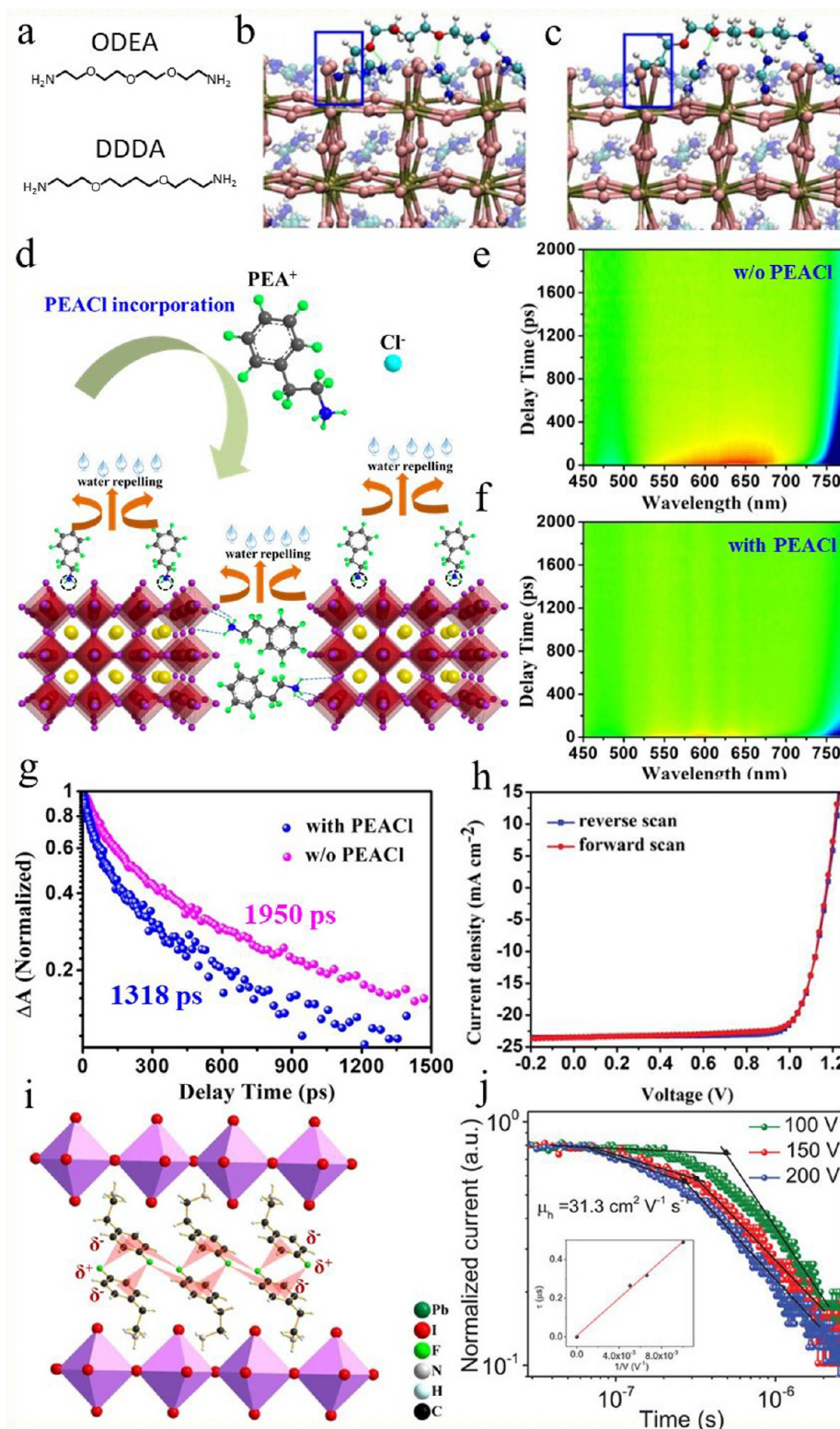


Figure 3. (a) The molecular structure of ODEA and DDDA. The molecular adsorptions on defect-contained surface of perovskites: (b) ODEA and (c) DDDA. (d) The defect passivation and water repellence of perovskites induced by PEACl modification. Contour plot TA spectra of perovskite films (e) without or (f) with PEACl. (g) Dynamic TA decay probed at the ground-state bleaching peak for perovskite films without or with PEACl modification. (h) $J-V$ curves of the champion PSC with PEACl passivation measured under forward and reverse scanning directions. (i) The optimized single crystal structure of $(\text{F-PEA})_2\text{PbI}_4$ (j) Normalized transient current curves of $(\text{F-PEA})_2\text{PbI}_4$ single crystal devices under various bias (inset shows the charge transit time verse the reciprocal of bias and the liner fit of the data). (a–c) Reproduced with permission from ref 37. Copyright 2019 Nature Publishing Group. (d–h) Reproduced with permission from ref 41. Copyright 2020 Wiley. (i and j) Reproduced with permission from ref 45. Copyright 2020 Wiley.

The modulation of alkyl chain length is also significant to balance the trade-off between defect passivation and interfacial charge collection. Considering that the linear alkyl chain is insulating, it is important to control the packing density thickness of ligands assembled on the perovskite surface, especially for the primary amines with unilateral amino groups. We further extended the alkyl chain length of amine ligands to 18 carbons. Oleylamine (OAm) with ultralong alkyl chains has often been regarded as a bottleneck that would hinder charge transfer. However, we made it possible by controlling the packing density of OAm ligands. Because the interaction force between OAm molecules is weaker than that of between OAm and perovskite, the anchoring of OAm (i.e., 300 ppm) is self-limited to a very thin monolayer (~ 2.46 nm in thickness) during thermal annealing of OAm-modified perovskite films. The OAm monolayer simultaneously served as an electron tunneling contact to facilitate electron transport from the perovskite layer to the electron transport layer (ETL) while blocking the holes, as a surface passivation layer to effectively suppress the interfacial charge recombination, and as a moisture-repelling barrier to protect the perovskite from water invasion (Figure 2d).¹² Long-chain amines remarkably improve the optoelectronic properties of perovskite films, for instance, decreasing the trap-state density by 2–4 orders, enhancing the carrier mobility from $1.6 \text{ cm}^2 \text{ V}^{-1} \text{ s}^{-1}$ to $3 \text{ cm}^2 \text{ V}^{-1} \text{ s}^{-1}$, and extending diffusion length from $\sim 1 \text{ }\mu\text{m}$ to $\sim 2 \text{ }\mu\text{m}$. As a result, an NREL-certified PCE of up to 22.3%, a surprisingly high FF exceeding 86% and excellent operational stability (i.e., operating at a maximum power point (MPP) for more than 1000 h under AM1.5G illumination with negligible loss of efficiency) have been achieved for inverted *p-i-n* structured PSCs with OAm-modification, which narrows the efficiency gap with conventional *n-i-p* structured PSCs.^{12,23}

Not just limited to organic–inorganic perovskites, Tang and co-workers modulated the quantum tunneling effect and optimized the interfacial charge transfer properties in inorganic CsPbBr₃-based PSCs by precisely regulating the alkyl chain length of the ligands, which facilitated interfacial charge extraction while minimizing the interfacial charge recombination loss (Figure 2e). The CsPbBr₃-based PSCs with 12-carbon long-chain ligands modification achieved a champion PCE of 10.85% with nearly unchanged PV performance under constant stresses of 80% relative humidity, 80 °C heating or continuous light irradiation in air.³¹ In addition to defect passivation and interfacial carrier dynamics optimization, modulation of the alkyl chain length is beneficial to regulating the crystal orientation, as well as phase distribution and stabilization of perovskites, especially for the low-dimensional perovskites and tin-based perovskites (Supporting Information Note 3).^{32–35}

2.2. Modulating the Molecular Structure of the “R” Core

Apart from alkyl chain length, the passivation efficacy of ligands on perovskites is also largely affected by the molecular structure of the “R” core. The charge distribution between the R core and the functional group tail should be carefully considered.^{20,36} Taking the amines as examples, the amino group can form both hydrogen bonds and coordination bonds with perovskite components. The competition between these two chemical interactions will influence the defect passivation efficacy. The rational molecular design of a series of primary amines, e.g., 2,2'-[oxybis(ethylenoxy)]diethylamine (ODEA) and 4,9-dioxa-1,12-dodecanediamine (DDDA), by introducing O atoms with strong electron-withdrawing properties in the

alkyl chain core has been proposed (Figure 3a). It is generally believed that the strength of coordination bond is stronger than that of hydrogen bond. Hence, for achieving robust defect passivation, forming coordination bonds between ligand molecules and perovskites is more desirable. Considering the competition between these two chemical interactions in the same amino group, it is favorable to weaken the electron-donating capability of N atoms via introducing another O atoms with strong electron-withdrawing properties in the alkyl chain core, thus lowering the chance of forming hydrogen bonds between amine molecules and organic cations in FAPbI₃ perovskite. For comparison, the inductive effect in DDDA is not that effective, because its N and O atoms are almost isolated from each other, resulting in the strongest hydrogen-bonding ability of the amino groups with perovskites (Figure 3b and 3c). In contrast, the ODEA effectively strengthens the coordination bonds formed with the defective perovskite surface for more robust defect passivation, which remarkably suppressed the nonradiative recombination (Supporting Information Note 4).³⁷

For primary amines with an insulating linear alkyl chain core, there is a substantive impact on the trade-off between defect passivation efficacy and charge transport property in ligand-modified perovskite films, especially when the length of linear alkyl chain is considerably long and the packing density of ligands is not suitably controlled. From a chemical point of view, one can consider to design and employ the secondary amines with amino group centered between two alkyl chains. In this case, once the amino groups interact with perovskites, the secondary amines prefer to be packed in a plane configuration, which would not significantly affect the interfacial charge transport property (Supporting Information Note 5).^{38,39} Another effective way is to utilize the amine analogues containing conjugated aromatic rings (e.g., benzene, fused rings and their derivatives), which show better charge transport characteristics and higher conductivity, owing to the delocalization effect of the electric orbitals (Supporting Information Note 6).⁴⁰ We deliberately substituted the linear alkyl chain connecting amine ligands with conjugated benzene rings, phenylethylammonium chloride (PEACl), which not only passivated negative charged defects at the surface and/or GBs via forming hydrogen bonds between PEA⁺ cations and undercoordinated I[−] ions but also facilitated charge transport from grains-to-grains and at related interfaces (Figure 3d–g). As a result, a high PCE of 22% for blade-coated PSCs under one sun illumination was attained (Figure 3h).⁴¹ As a bonus, the conjugated amines show great potential to stabilize black-phase FA-dominant perovskites with an optimal bandgap of ~ 1.51 eV, possibly benefiting from the hydrophobicity of conjugated cations, as well as strain management induced by π – π stacking and favorable steric arrangement on the perovskite surface.⁴² The interaction between perovskites and conjugated ligands can form favorable dipole moments at relevant interfaces, which modifies the interfacial carrier dynamics and improve the device stability (Supporting Information Note 7).^{43,44} Li et al. demonstrated that employing F-PEA (fluorophenethylammonium) ligands, in which the electron-deficient F atoms form supramolecular electrostatic interaction with neighboring benzene rings, can induce dipole interaction and enhance the π – π stacking between benzene rings by aligning the benzene rings in the same direction (Figure 3i). In this case, the intermolecular interaction and cross-linking between the bulky organic spacers

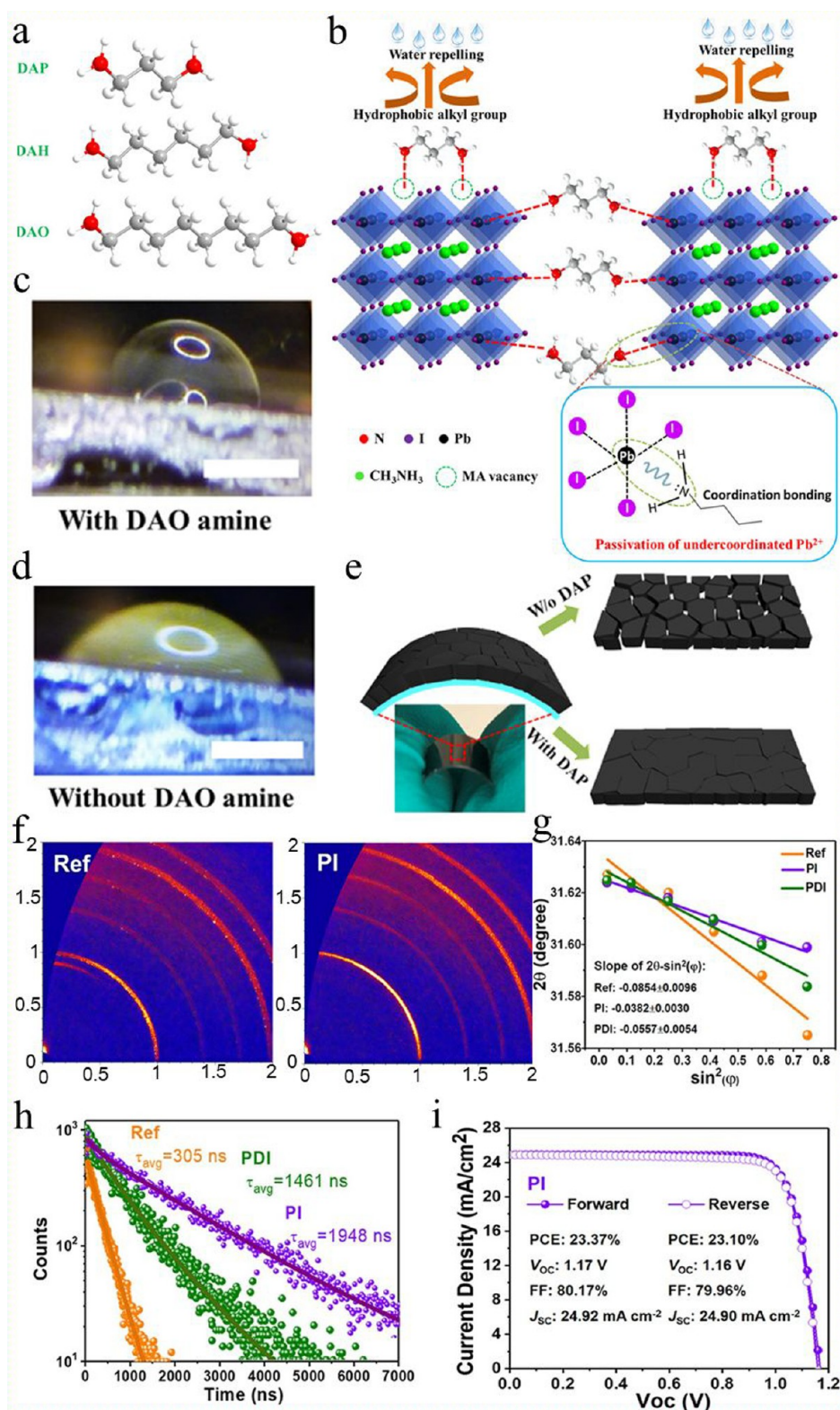


Figure 4. (a) Chemical structures of BAA additives. (b) Defect passivation, crystal cross-linking, and water repellence induced by BAA modification. Contact angle measurement of a water droplet on MAPbI₃ thin films (c) with or (d) without incorporated BAA additive. (e) The morphology change of the perovskite films deposited on a flexible ITO-PET substrate after the bending test. (f) Two-dimensional GIWAXS patterns of reference and PI-modified perovskite films. (g) Corresponding diffraction strain data of perovskite films as a function of $\sin^2 \varphi$. (h) Time-resolved photoluminescence plots of perovskite films of different perovskite films as indicated. (i) $J-V$ curves of the PI-treated device measured under different scanning directions. (a–e) Reproduced with permission from ref 2. Copyright 2019 American Association for the Advancement of Science. (f–i) Reproduced with permission from ref 5. Copyright 2020 American Chemical Society.

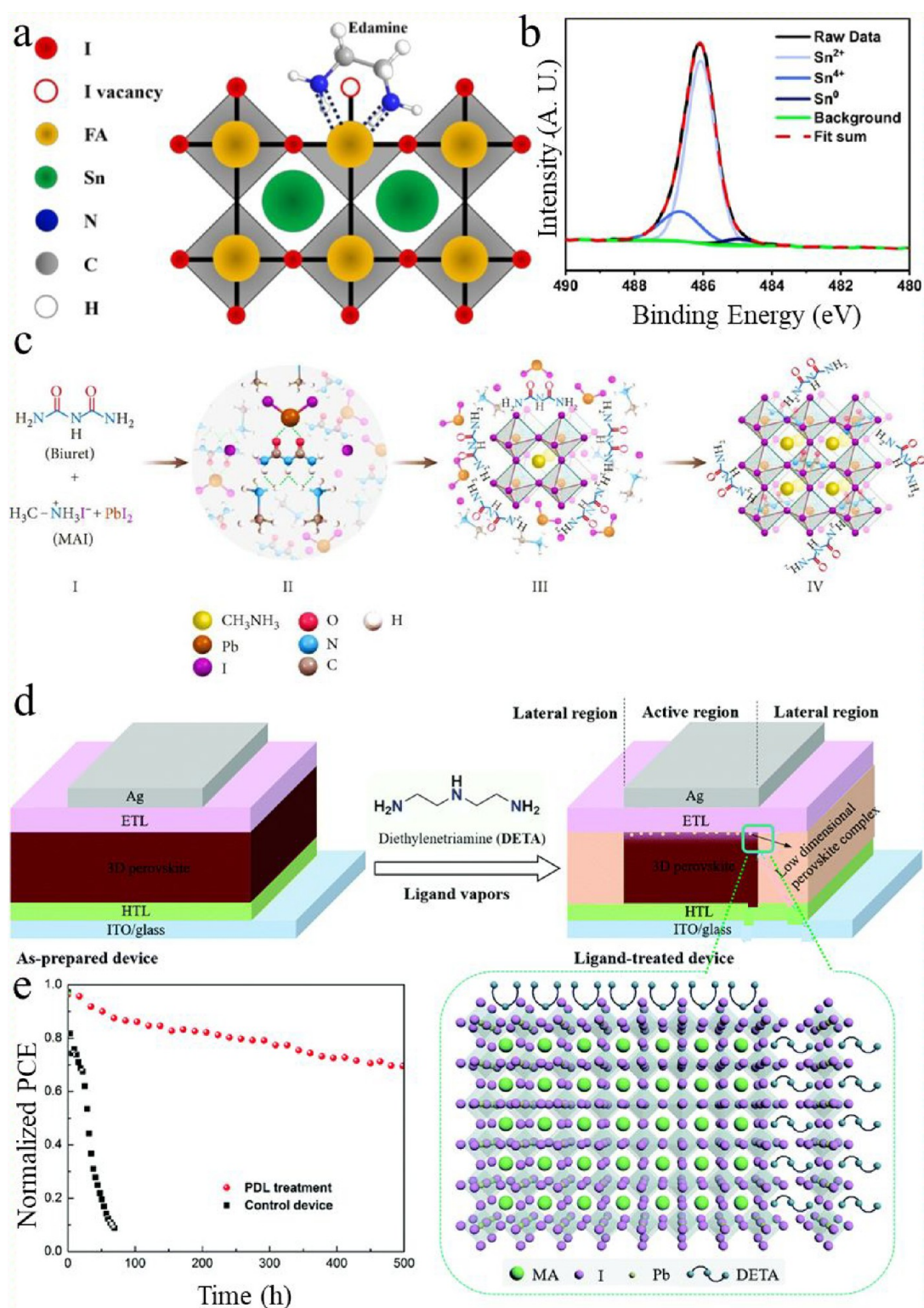


Figure 5. (a) Passivation of iodide vacancies and stabilization of undercoordinated Sn^{2+} by EDA molecules. (b) Narrow XPS spectra of $\text{Sn } 3d_{5/2}$ for 0.05 mM edamine-passivated $\text{FA}_{0.98}\text{EDA}_{0.01}\text{SnI}_3$ samples. (c) The biuret additive-assisted growth of MAPbI_3 perovskite. (d) The PDL treatment process and the relevant device configuration, the molecular structure of DETA, and a possible model for DETA interaction with the MAPbI_3 cage. (e) MPP tracking over 500 h of unencapsulated devices under continuous 1 sun illumination. (a and b) Reproduced with permission from ref 49. Copyright 2019 American Chemical Society. (c) Reproduced with permission from ref 50. Copyright 2020 American Association for the Advancement of Science. (d and e) Reproduced with permission from ref 51. Copyright 2018 Royal Society of Chemistry.

was significantly strengthened, which benefited blocking ion migration paths and improved the intrinsic stability of perovskites. In addition, the carrier mobility of $(\text{F-PEA})_2\text{PbI}_4$

single crystal is significantly enhanced to $31.3 \text{ cm}^2 \text{ V}^{-1} \text{ s}^{-1}$, which is much larger than that of $(\text{PEA})_2\text{PbI}_4$ single crystal (Figure 3j).⁴⁵

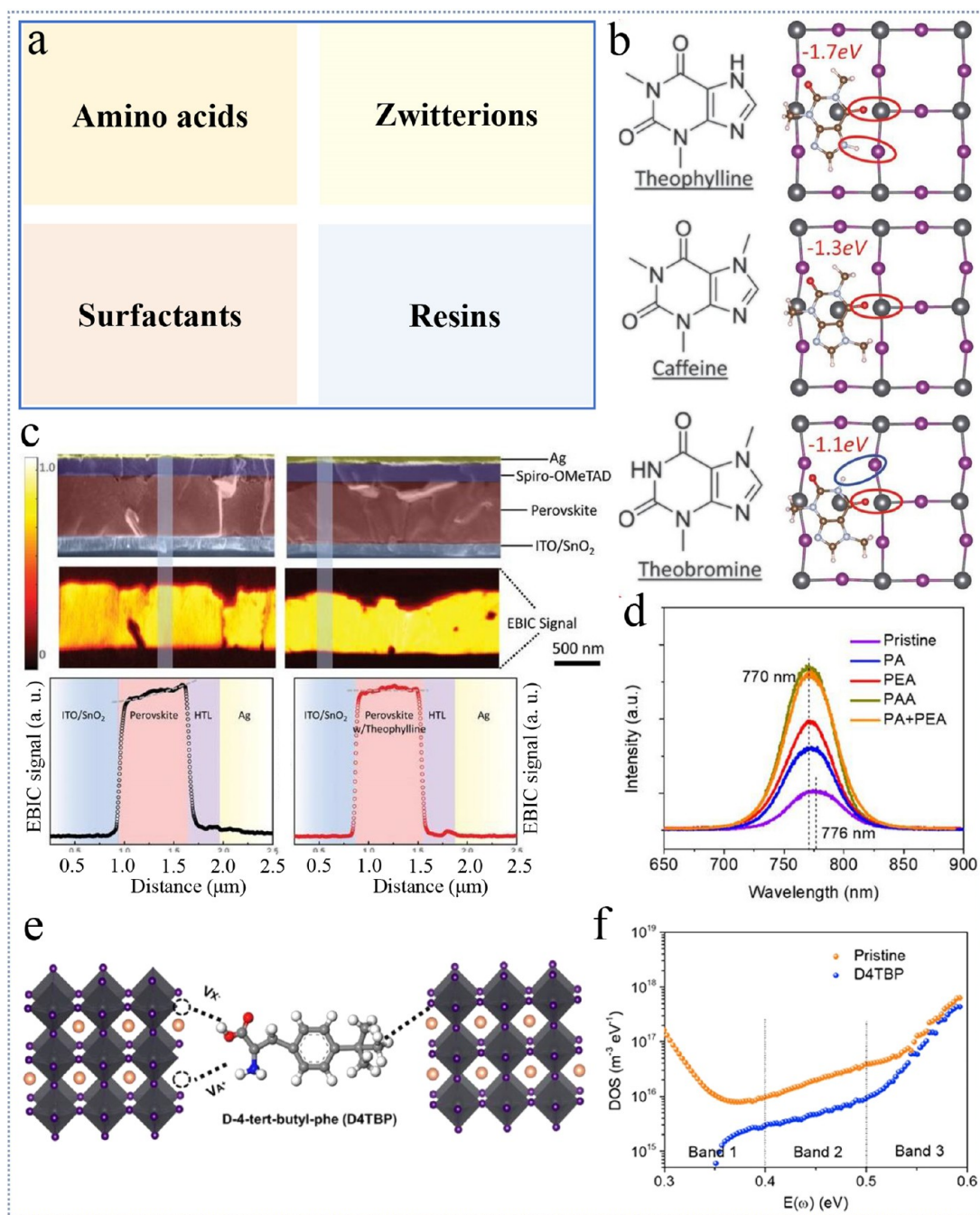


Figure 6. (a) Summary of several representative “all-in-one” ligands used in high-performance PSCs. (b) Theoretical models of perovskite with molecular surface passivation of PbI₂ antisite by theophylline, caffeine, and theobromine. (c) Cross-sectional SEM images and corresponding EBIC images and line profiles of PSCs without (left) or with (right) theophylline treatment. (d) PL spectra of perovskite films with different passivation layers. (e) The D4TBP passivation effect on different defect sites in perovskites. (f) Trap density in pristine and D4TBP-passivated PSCs. (b and c) Reproduced with permission from ref 27. Copyright 2019 American Association for the Advancement of Science (AAAS). (d–f) Reproduced with permission from ref 54. Copyright 2019 American Chemical Society.

2.3. Tuning the Number of Unitary Functional Groups

Ligands with single functional groups at the tail exhibit controllable defect passivation efficacy, but only limited anchoring capacity on perovskite films. In contrast, ligands with double, triple, quadruple, or even more functional groups could serve as a claw to strongly bond with perovskites, thus further enhancing the defect passivation effect.^{46–48} We proposed the versatile concept of “bilateral amine (BAA) passivation” and designed a series of “NH₂-R-NH₂” molecules,

i.e., 1,3-diaminopropane (DAP), 1,6-diaminohexane (DAH), and 1,8-diaminooctane (DAO), that strongly bond on various perovskite compositions to improve the efficiency and stability of PSCs (Figure 4a).² Specifically, both -NH₂ tails are targeted to anchor on the perovskite grain surface while exposing the linking hydrophobic carbon chain, which is capable of simultaneously passivating the surface defects, forming a moisture-repelling barrier on the perovskite grains, cross-linking adjacent grains for improved film compactness, reinforcing the grain boundaries, and improving the mechan-

ical strength of the perovskite film (Figure 4b–e). Blade-coated PSCs with DAP modification achieved a PCE close to 22%. The robust passivation effect also contributed to achieving over 23% efficiency under weak light (0.3 sun) illumination, highlighting the potential of additive-assisted defect passivation toward new-generation indoor PVs.^{2,6}

Strain management of perovskites has been demonstrated as a key factor to affect the efficiency and stability of PSCs. Li et al. used a bifunctional molecule, piperazinium iodide (PI), which links both neutral R_2NH (electron donor) and positively charged $R_2NH_2^+$ (electron acceptor) functional groups on the same six-membered ring, to modify the surface of the perovskite film. Grazing-incidence wide-angle X-ray scattering (GIWAXS) results show that PI-modified perovskite film has better crystallinity compared with the reference film (Figure 4f), and the residual lattice strain on the surface of the PI-modified perovskite film is effectively released (Figure 4g), which is conducive to inhibiting nonradiative recombination (Figure 4h) and makes the perovskites intrinsically more stable. In addition, the PI-modified perovskite film became more n-type, which enabled more efficient energy transfer at the perovskite/ETL interface. Finally, the optimized inverted device achieved a record PCE of 23.37% (a certified value of 22.75%) and a high V_{oc} of 1.17 V (Figure 4i).⁵

Tin-based perovskites have small optical bandgaps and high carrier mobilities, which show great potential to break the SQ limit. However, Sn^{2+} is easily oxidized to Sn^{4+} , which leads to a self-p-type doping effect and reduces device efficiency and stability. Ligands with multiple functional groups can interact with undercoordinated Sn^{2+} ions, to some extent retard oxidation Sn^{2+} oxidation. Kamarudin et al. used 1,2-diaminoethane (DAE) to passivate the surface defects of a tin-based perovskite (Figure 5a), which also inhibited Sn^{2+} oxidation (Figure 5b), thus increasing the V_{oc} by 100 mV to 0.59 V and obtained a PCE of 10.18% for $FA_{0.98}EDA_{0.01}SnI_3$ -based PSCs.⁴⁹ Lv et al. incorporated a series of carbamide molecules (i.e., urea, biuret, or triuret) consisting of triple amine substituents into the perovskite precursor to robustly eliminate the bulk and surface defects. The interaction between the functional groups (i.e., $-C=O$ and $-NH_2$) in biuret and perovskite precursor components (i.e., PbI_2 and MAI) not only facilitated the growth of large-sized grains but also passivated crystallographic defects (Figure 5c) and contributed greatly to reduce carrier recombination loss. Triuret is easier to anchor on the perovskite surface to form a dendritic triuret–perovskite intermediate layer, which facilitates the electron transfer from the perovskite layer to the ETL. As a result, a champion efficiency of 21.6% was achieved in $MAPbI_3$ -based PSCs with an inverted structure by combining biuret and triuret additives.⁵⁰

Dealing with “poor devices” during any future mass-production process is still an open question. Zhang et al. proposed vapor treatment of the completed device based on $MAPbI_3$ perovskites with diethylenetriamine (DETA) ligands featuring triple amino substituents. This postdevice ligand (PDL) treatment will both completely convert the 3D perovskite in the nonworking area into low-dimensional $(DETA)_2(CH_3NH_3)_{n-1}Pb_nI_{3n+1}$ perovskite to protect the inner 3D components and interact with the perovskite in the working area for passivating defects (Figure 5d). The PDL treatment saves “poor devices”, reproducibly improving PCEs by more than 5% and prolonging the lifespan of devices in

ambient condition even without encapsulation (Figure 5e) (Supporting Information Note 8).⁵¹

To take full advantage of ligand molecules featuring multiple unitary functional groups, other factors such as molecule size, length, flexibility, and steric hindrance of the backbone should be carefully considered and designed, to maximize the interaction sites and strength between the perovskites host and exotic ligands guest. Ligands with the same functional groups but different molecular structures may exhibit different interaction behavior and capability with perovskite species, thus making additives combination feasible and promising. In some cases, the additives combination can synergistically improve the crystalline and optoelectronic properties of the perovskite films, as well as optimizing the interfacial carrier dynamics of PV devices.

2.4. Designing “All-in-One” Multidentate Ligands

The flexible structure of ligands permits infinite possibilities of evolving to more advanced molecules. Besides coordination bonding, hydrogen bonding and ionic interaction, the surface chelation of perovskite via the formation of multiple, strong chelate bonds between undercoordinated Pb sites and multidentate ligands (e.g., amino acids, zwitterions, amphiphilic surfactants, resin, etc.) is one of the most effective strategies to realize a robust defect passivation effect and strengthen the intrinsic stability of perovskite materials.^{52,53}

Figure 6a illustrates several representative “all-in-one” ligands used in fabricating high-performance PSCs. Wang et al. found that different functional groups in theophylline, caffeine, and theobromine can affect the interaction between passivation molecules and lead–iodine antisite defects in perovskite. When N–H and C=O were designed to be an optimal configuration in a molecule like theophylline, the hydrogen bond formation between N–H and iodine could strengthen the bonding of primary C=O with the Pb–I antisite defect (i.e., an interaction energy as strong as -1.7 eV), which could maximize the surface defect passivation effect (Figure 6b). Obviously, the N–H functional group indeed works efficiently to stabilize the iodine, while simultaneously changes the surrounding electron density and promote the defect passivation efficacy of C=O functional groups. A device with theophylline treatment exhibited higher electron-beam-induced current (EBIC) and minimal decay from the hole transport layer to the SnO_2 –perovskite interface compared with the reference device, suggesting facilitated charge transfer and suppressed nonradiative recombination for the former (Figure 6c). After theophylline treatment, a stabilized PCE of 22.6% was achieved (Supporting Information Note 9).²⁷

Amino acids consisting of an amine group and carboxyl group can exert a dual-passivation effect, which have been widely employed in perovskite PVs. Huang and colleagues studied the passivation effect on perovskites of carboxyl group, amine group, and both carboxyl and amine groups using phenylpropionic acid (PA), phenylethylamine (PEA), and phenylalanine (PAA). The PL test showed that the carboxyl and amine groups effectively passivate positively and negatively charged defects, respectively. The PAA-passivated perovskite film had a similar PL intensity to the PA + PEA sample, which can be attributed to the presence of the two functional groups (Figure 6d). The D4TBP amino acid molecule combining all the structural merits of specific passivation groups was designed to maximize the defect passivation effect and efficacy. The *tert*-butyl group (on the benzene ring) enhances the

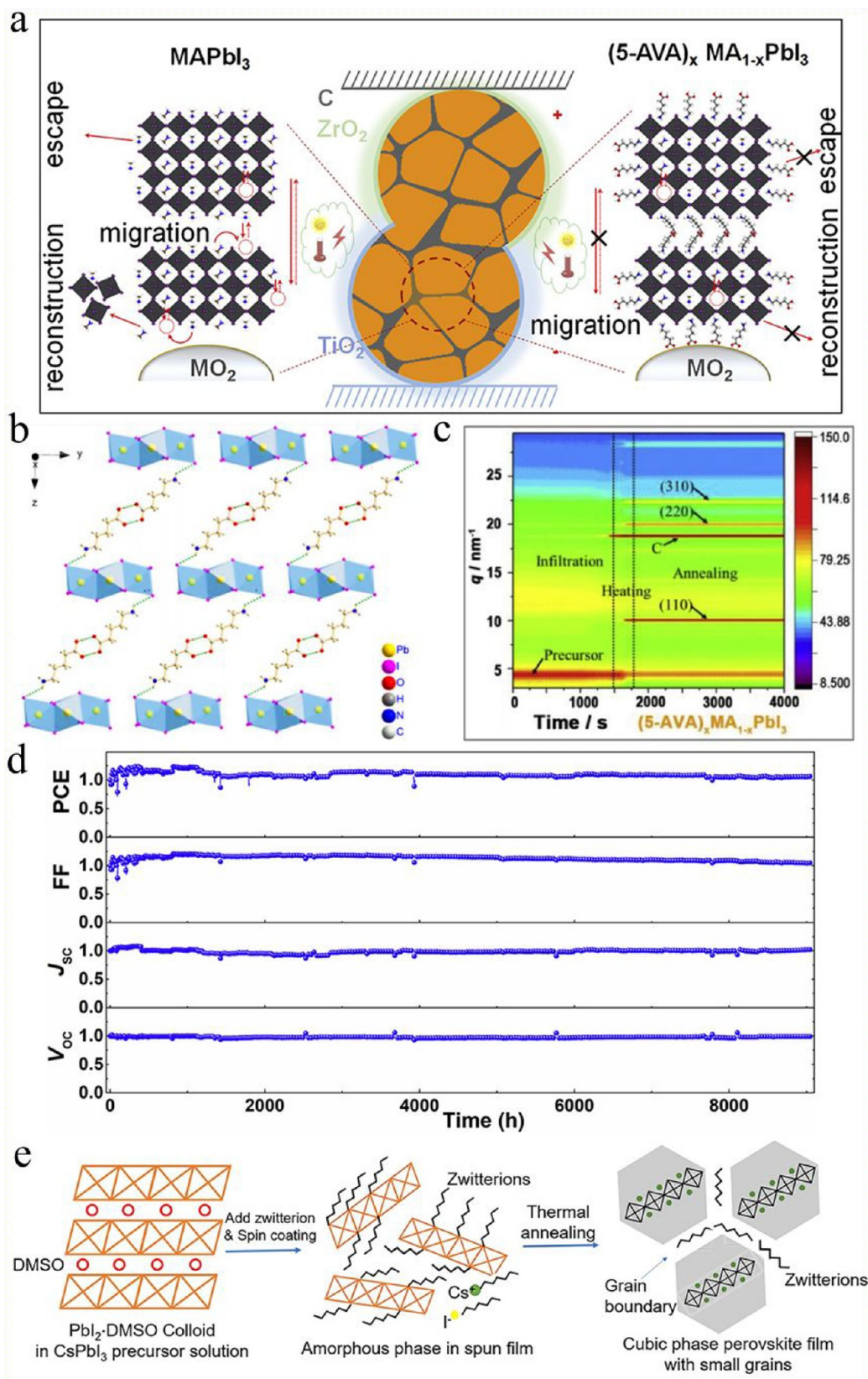


Figure 7. (a) Structures of MAPbI_3 and $(5\text{-AVA})_x\text{MA}_{1-x}\text{PbI}_3$ in triple-mesoscopic layers and the process of materials decomposition and ionic migration under light, heat and electronic bias. (b) The schematic illustration of partial interaction between 5-AVAI and PbI_2 . (c) *In-situ* GIWAXS tracking of the $(5\text{-AVA})_x\text{MA}_{1-x}\text{PbI}_3$ crystallization process in the mesoscopic structure. (d) The tracking of photovoltaic parameters for printable mesoscopic PSCs under operational conditions for over 9000 h. (e) The interactions between zwitterions and CsPbI_3 perovskite species and the corresponding phase stabilization mechanism. (a–d) Reproduced with permission from ref 7. Copyright 2020 Elsevier. (e) Reproduced with permission from ref 24. Copyright 2017 Elsevier.

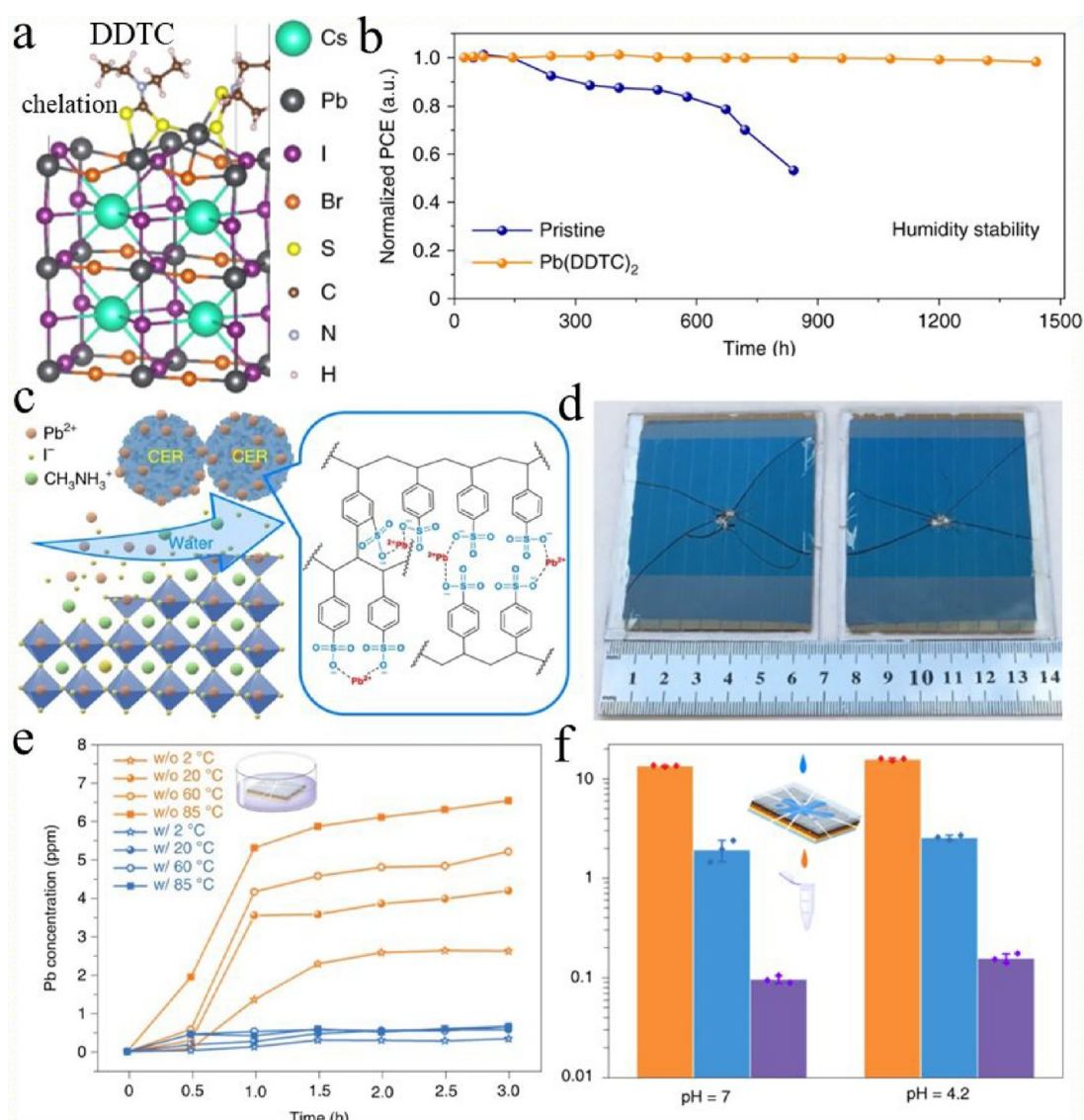


Figure 8. (a) Atomic structure of optimized CsPbI₂Br (001) with the Pb(DDTC)₂ molecule chelating on the surface. (b) PCE evolution of the pristine and Pb(DDTC)₂-chelated CsPbI₂Br devices without encapsulation. (c) Schematic of how CERs prevent lead leakage due to the strong ionic interaction between Pb²⁺ in decomposed perovskites and multisulfonate groups in CERs. (d) The photos of mechanically damaged perovskite-based PV mini-modules. (e) Water-soaking test results for the damaged mini-modules without or with a CER coating layer. (f) Water-dripping test results for the damaged mini-modules without or with a CER coating layer: orange, control mini-modules without a CER layer encapsulated by a glass slide; blue, mini-modules with a back CER layer encapsulated by a glass slide; purple, mini-modules with both front and back CER layers encapsulated by a polypropylene sheet. (a and b) Reproduced with permission from ref 58. Copyright 2020 Nature Publishing Group. (c–f) Reproduced with permission from ref 59. Copyright 2020 Nature Publishing Group.

electron-donating ability of the benzene ring, as compared with PAA, thereby more effectively passivating the iodine-based defect and undercoordinated Pb²⁺ (Figure 6e and 6f). A PCE of 21.4% for a 1.57 eV bandgap PSCs was obtained, corresponding to only a very small V_{oc} loss of 0.34 V.⁵⁴

Different molecular structures can modulate the molecular interaction between the passivation agent and the crystal defect of perovskites (Supporting Information Note 10).⁵⁵ Han and colleagues incorporated the bifunctional 5-ammoniumvaleric acid (S-AVAI) into perovskites, which stabilized the GBs and interfaces via a strong molecular interaction between SAVAI and MAPbI₃ perovskite. The S-AVAI could attach on the surface of MAPbI₃ grains with their ammonium groups and tailor the grain sizes of MAPbI₃. The carboxyl groups then interact via the strong hydrogen bond with either another S-

AVAI on an adjacent grain or the metal oxide substrates, enabling tight connection between grains, or grains and the metal oxide substrate. Moreover, 5-AVAI inhibits the loss of MAI and restricts ion migration at MAPbI₃ GBs and the interfaces between MAPbI₃ and the mesoscopic layer (Figure 7a–c). No performance attenuation was observed when the devices were tracked under MPP condition for more than 9,000 h (Figure 7d).⁷ In addition, the effects of ligand molecule hydrophilicity and hydrophobicity on perovskite film formation have been investigated (Supporting Information Note 11).^{17,26}

Ligand molecules containing S-donor have sulfur-bearing lone electron pairs that can effectively passivate Pb²⁺ dangling bonds and exhibit a stronger coordination bonding capability with perovskites than O-donor counterparts. Several sulfonic

zwitterions ligands, a type of neutral molecule with both positive and negative electrical charges, have been shown to demonstrate all-in-one capability in terms of modulating the crystallization kinetics and stabilizing the desirable phase structure of perovskite films, and more encouragingly, passivating multivacancies defects in solution-processed perovskites simply by introducing one type of ligand molecules.^{9,10} Huang and colleagues pioneered the concept of “passivation of multi-vacancies defects by using zwitterions ligands”. Such a zwitterionic molecule with separated positive and negative ions has the advantage of self-adaptive selection of defects with opposite charges for targeted passivation and is not limited by either complicated defect composition or distribution at the surface of the perovskite film (Supporting Information Note 12).^{9,56} Functioning not only as effective defect passivators, zwitterionic ligands, e.g., 3-(decyldimethylammonium)-propane-sulfonate inner salt (DPSI), tetradecyl dimethyl (3-sulfopropyl) ammonium hydroxide inner salt (TAH), and L-alanine, have been incorporated in perovskite inks to modulate the crystal growth and crystallization of perovskite films.^{10,19,57} This improved the film quality and, more interestingly, enabled room temperature blade-coating of high-quality perovskite films with arbitrary compositions. Sulfobetaine zwitterions were also reported to impede the crystallization of CsPbI₃ perovskite films via electrostatic interaction between the ligand molecules and perovskite colloids, thereby reducing the grain size and increasing the surface energy of the grains (Figure 7e). This is conducive to stabilizing black-phase CsPbI₃ perovskite film at room temperature, with derived PSCs exhibiting a stabilized PCE of 11.4%.²⁴

A molecularly tailored, mechanically tough and self-healing ligand containing N-, S-, and O-based functional groups, i.e., thiourea-triethylene glycol, was incorporated into a polycrystalline perovskite thin film to form a composite with a bicontinuous interpenetrating network (Supporting Information Note 13). He et al. developed a chelation strategy for effectively healing surface undercoordinated defects of inorganic CsPbI₂Br perovskite, in which diethyldithiocarbamate (DDTC) molecules coordinate to surface Pb sites via strong bidentate chelate bonding (Figure 8a). The DDTC-modified surface exhibited very weak adsorption strength of water to perovskite, suggesting that the chelation strategy can be a promising approach to stabilize perovskite under humid environments and enhance the overall performance. Hence, CsPbI₂Br PSCs with DDTC chelation can maintain 98% of the initial efficiency when stored at room temperature for 1400 h (Figure 8b).⁵⁸ The chelation effect of multidentate ligands is also advantageous to minimize lead leakage from water-soluble lead halide perovskite-based devices. Chen et al. designed a low-cost, chemically robust cation-exchange resin (CER) to effectively prevent lead leakage from damaged PSCs modules under extreme weather conditions via a chelation strategy (Figure 8c). After putting each damaged mini-module (Figure 8d) into 200 mL of deionized water at different temperatures for 1 h, the lead concentration in the water from the mini-modules without a CER coating increased dramatically, while the damaged mini-modules with a CER coating largely minimized lead leakage regardless of temperature change (Figure 8e). After attack by hail, the average lead concentration in contaminated water of damaged mini-modules without a CER layer was 13.24 ± 0.25 ppm, while this value was greatly

reduced to 1.92 ± 0.46 ppm for the devices with a CER layer (Figure 8f).⁵⁹

3. CONCLUSION AND OUTLOOK

We have comprehensively elucidated how custom molecular design of ligands with desirable structures and properties can closely interact with the soft perovskite lattice and robustly heal the intrinsic imperfections of polycrystalline perovskite films. Moreover, we summarized feasible rules that guide the rational design of multifunctional ligands (i.e., organic moieties R core and functional groups) for improving the efficiency and stability of perovskite PVs. We insightfully explored the multifunctionalities of ligand molecules via ingenious and flexible molecular design (Supporting Information Note 14).

While much fruitful achievement has been achieved with custom ligands and perovskites, and a prosperous future can be foreseen, further research efforts are needed to design more advanced and perfect ligand molecules to tap the omnibearing potential of magic perovskites. Accordingly, we propose three major research implications and provide some insightful perspectives (Figure 9).

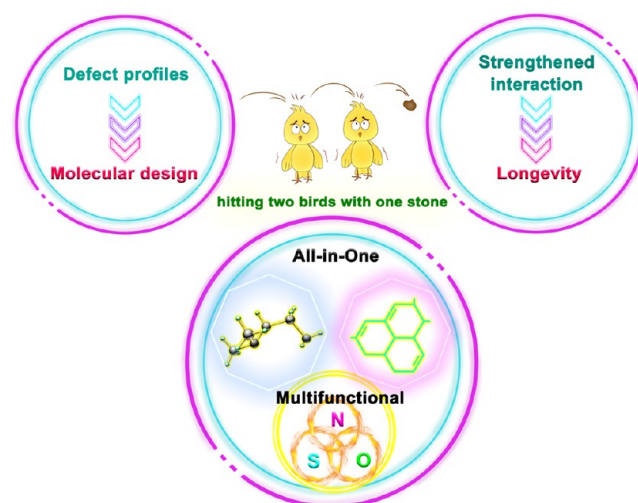


Figure 9. Future research implications of optimizing the molecular design strategy.

First, a fundamental understanding, from a materials design point of view, should be achieved through a combination of in-depth characterization and theoretical calculation, especially for the types and profiles of defects, the origins of V_{oc} losses, the locations and distributions of anchored ligands, and the multifunctionalities of ligand molecules. This would guide the ingenious molecular design of more advanced and ideal ligand molecules that perfectly fit with the perovskite matrix. A correlation between the molecular structure of ligands and device performance must be clarified.

Second, the chemical interaction between perovskites and ligand molecules should be further strengthened, which is desirable to improve defect passivation efficacy and longevity. The widely adopted coordination bonding formation between neutral Lewis base-typed ligands with N-, O-, S-, and P-donors and undercoordinated Pb²⁺ ions in polycrystalline perovskites exhibited stronger interaction strength than that of ionic bonding and hydrogen bonding formed between charged ligands and the charged components in perovskites. Surface chelation bonding between multiple functional groups and one

central undercoordinated metal ion represents the strongest interaction with perovskites, which can be attributed to the formation of very stable, claw-like ring compounds. Thus, the design of innovative multidentate ligands with improved affinity for perovskites will further improve the defect passivation efficiency and intrinsic stability (Supporting Information Note 15).

Third, “hitting two birds with one stone” is both a principle and incentive for designing multifunctional “all-in-one” ligands, which can intelligently heal multiple types of defects at the bulk and/or surface of perovskite films, rather than relying on the combination of two or more molecules. One can utilize the machine learning strategy to boost the screening and advance the discovery of novel multifunctional ligands. For targeted “all-in-one” ligands, several factors related to the core and tail of the specific molecule need to be carefully considered, including the packing density, anchoring site(s), steric hindrance, charge distribution, conductivity, hydrophilicity, hydrophobicity, intramolecular interactions, etc. The incorporation of double, triple, quadruple, or even more functional groups is desirable to achieve a more robust defect passivation effect, which integrates several types of chemical interaction and/or bonding. However, attention should also be paid to the trade-off of introducing functional groups, either positive or negative (Supporting Information Note 16). Considering the complicated spatial distribution of defects in perovskite films, an ideal ligand of suitable molecular length and/or size should be capable of achieving self-adaptive selection of defects with matched moieties for targeted passivation. Compared with the ligands with aliphatic chains that are not efficient enough to conduct the charges, the conjugated ligands with aromatic rings and/or fused rings are more desirable to achieve a trade-off between defect passivation efficacy and charge transport property in ligand-modified perovskite films, especially for PQDs-based analogues (Supporting Information Note 17).

■ ASSOCIATED CONTENT

SI Supporting Information

The Supporting Information is available free of charge at <https://pubs.acs.org/doi/10.1021/accountsmr.1c00099>.

Extended discussion about imperfections in perovskites, molecular design of ligands (alkyl chain length, “R” core, number of functional groups and multifunctionality), and research outlook (PDF)

■ AUTHOR INFORMATION

Corresponding Authors

Lianzhou Wang – Nanomaterials Centre, School of Chemical Engineering and Australian Institute for Bioengineering and Nanotechnology, The University of Queensland, Brisbane, QLD 4072, Australia; orcid.org/0000-0002-5947-306X; Email: l.wang@uq.edu.au

Wu-Qiang Wu – MOE Key Laboratory of Bioinorganic and Synthetic Chemistry, School of Chemistry, Sun Yat-sen University, Guangzhou 510006, P. R. China; orcid.org/0000-0001-5414-5668; Email: wuwq36@mail.sysu.edu.cn

Authors

Meifang Yang – MOE Key Laboratory of Bioinorganic and Synthetic Chemistry, School of Chemistry, Sun Yat-sen University, Guangzhou 510006, P. R. China

Tian Tian – MOE Key Laboratory of Bioinorganic and Synthetic Chemistry, School of Chemistry, Sun Yat-sen University, Guangzhou 510006, P. R. China

Wenhui Feng – MOE Key Laboratory of Bioinorganic and Synthetic Chemistry, School of Chemistry, Sun Yat-sen University, Guangzhou 510006, P. R. China

Complete contact information is available at:

<https://pubs.acs.org/doi/10.1021/accountsmr.1c00099>

Notes

The authors declare no competing financial interest.

Biographies

Meifang Yang is a Ph.D. candidate at Sun Yat-sen University. Her research interests lie in efficient and stable perovskite photovoltaics.

Tian Tian received her Ph.D. degree from the University of Shanghai for Science and Technology in 2020. Her research interests lie in the fabrication of functional semiconducting crystals and their applications in optoelectronic devices.

Wenhui Feng is a Ph.D. candidate at Sun Yat-sen University. His research interests lie in perovskite materials and devices.

Lianzhou Wang is a Professor at the School of Chemical Engineering, and Director of Nanomaterials Centre, the University of Queensland (UQ), Australia. He received his Ph.D. degree from the Chinese Academy of Sciences in 1999. Before joining UQ in 2004, he worked at two national institutes of Japan (NIMS and AIST) for five years. His research interests include the design and application of semiconductor nanomaterials for solar energy conversion and storage systems including photocatalysis and photoelectrochemical devices.

Wu-Qiang Wu received his Ph.D. degree from the University of Melbourne in 2017. His research interests lie in the design and fabrication of functional optoelectronic materials for solar energy conversion, such as dye- and quantum dot-sensitized solar cells and perovskite solar cells.

■ ACKNOWLEDGMENTS

The authors acknowledge financial support from the National Key R&D Program of China (2019YFB1503200), the National Natural Science Foundation of China (22005355), and the Guangdong Basic and Applied Basic Research Foundation (2019A1515110770). L. Wang acknowledges the financial support from ARC through its Discovery Program.

■ REFERENCES

- (1) NREL. *Best Research-Cell Efficiency Chart*; U.S. Department of Energy, 2021. <https://www.nrel.gov/pv/cell-efficiency.html> (accessed 02–15–2021).
- (2) Wu, W.-Q.; Yang, Z.; Rudd, P. N.; Shao, Y.; Dai, X.; Wei, H.; Zhao, J.; Fang, Y.; Wang, Q.; Liu, Y.; Deng, Y.; Xiao, X.; Feng, Y.; Huang, J. Bilateral Alkylamine for Suppressing Charge Recombination and Improving Stability in Blade-Coated Perovskite Solar Cells. *Sci. Adv.* **2019**, *5*, No. eaav8925.
- (3) Xue, J.; Wang, R.; Chen, X.; Yao, C.; Jin, X.; Wang, K.-L.; Huang, W.; Huang, T.; Zhao, Y.; Zhai, Y.; Meng, D.; Tan, S.; Liu, R.; Wang, Z.-K.; Zhu, C.; Zhu, K.; Beard, M. C.; Yan, Y.; Yang, Y. Reconfiguring the band-edge states of photovoltaic perovskites by conjugated organic cations. *Science* **2021**, *371*, 636–640.
- (4) Zheng, X.; Alsalloum, A. Y.; Hou, Y.; Sargent, E. H.; Bakr, O. M. All-Perovskite Tandem Solar Cells: A Roadmap to Uniting High Efficiency with High Stability. *Acc. Mater. Res.* **2020**, *1*, 63–76.
- (5) Li, F.; Deng, X.; Qi, F.; Li, Z.; Liu, D.; Shen, D.; Qin, M.; Wu, S.; Lin, F.; Jiang, S. H.; Zhang, J.; Lu, X.; Lei, D.; Lee, C. S.; Zhu, Z.; Jen,

- A. K. Regulating Surface Termination for Efficient Inverted Perovskite Solar Cells with Greater Than 23% Efficiency. *J. Am. Chem. Soc.* **2020**, *142*, 20134–20142.
- (6) Wu, W. Q.; Rudd, P. N.; Ni, Z.; Van Brackle, C. H.; Wei, H.; Wang, Q.; Ecker, B. R.; Gao, Y.; Huang, J. Reducing Surface Halide Deficiency for Efficient and Stable Iodide-Based Perovskite Solar Cells. *J. Am. Chem. Soc.* **2020**, *142*, 3989–3996.
- (7) Mei, A.; Sheng, Y.; Ming, Y.; Hu, Y.; Rong, Y.; Zhang, W.; Luo, S.; Na, G.; Tian, C.; Hou, X.; Xiong, Y.; Zhang, Z.; Liu, S.; Uchida, S.; Kim, T.-W.; Yuan, Y.; Zhang, L.; Zhou, Y.; Han, H. Stabilizing Perovskite Solar Cells to IEC61215:2016 Standards with over 9,000-h Operational Tracking. *Joule* **2020**, *4*, 2646–2660.
- (8) Chen, C.-H.; Lou, Y.-H.; Wang, K.-L.; Su, Z.-H.; Dong, C.; Chen, J.; Shi, Y.-R.; Gao, X.-Y.; Wang, Z.-K. Ternary Two-Step Sequential Deposition Induced Perovskite Orientational Crystallization for High-Performance Photovoltaic Devices. *Adv. Energy Mater.* **2021**, *11*, 2101538.
- (9) Zheng, X.; Chen, B.; Dai, J.; Fang, Y.; Bai, Y.; Lin, Y.; Wei, H.; Zeng Xiao, C.; Huang, J. Defect passivation in hybrid perovskite solar cells using quaternary ammonium halide anions and cations. *Nat. Energy* **2017**, *2*, 17102.
- (10) Zheng, X.; Deng, Y.; Chen, B.; Wei, H.; Xiao, X.; Fang, Y.; Lin, Y.; Yu, Z.; Liu, Y.; Wang, Q.; Huang, J. Dual Functions of Crystallization Control and Defect Passivation Enabled by Sulfonic Zwitterions for Stable and Efficient Perovskite Solar Cells. *Adv. Mater.* **2018**, *30*, 1803428.
- (11) Jiang, X.; Zang, Z.; Zhou, Y.; Li, H.; Wei, Q.; Ning, Z. Tin Halide Perovskite Solar Cells: An Emerging Thin-Film Photovoltaic Technology. *Acc. Mater. Res.* **2021**, *2*, 210–219.
- (12) Wu, W.-Q.; Zhong, J.-X.; Liao, J.-F.; Zhang, C.; Zhou, Y.; Feng, W.; Ding, L.; Wang, L.; Kuang, D.-B. Spontaneous surface/interface ligand-anchored functionalization for extremely high fill factor over 86% in perovskite solar cells. *Nano Energy* **2020**, *75*, 104929.
- (13) Li, B.; Di, H.; Chang, B.; Yin, R.; Fu, L.; Zhang, Y. N.; Yin, L. Efficient Passivation Strategy on Sn Related Defects for High Performance All-Inorganic CsSnI₃ Perovskite Solar Cells. *Adv. Funct. Mater.* **2021**, *31*, 2007447.
- (14) Zhou, Y.; Wang, F.; Cao, Y.; Wang, J.-P.; Fang, H.-H.; Loi, M. A.; Zhao, N.; Wong, C.-P. Benzylamine-Treated Wide-Bandgap Perovskite with High Thermal-Photostability and Photovoltaic Performance. *Adv. Energy Mater.* **2017**, *7*, 1701048.
- (15) Nishimura, K.; Kamarudin, M. A.; Hirotsu, D.; Hamada, K.; Shen, Q.; Iikubo, S.; Minemoto, T.; Yoshino, K.; Hayase, S. Lead-free tin-halide perovskite solar cells with 13% efficiency. *Nano Energy* **2020**, *74*, 104858.
- (16) Jang, G.; Ma, S.; Kwon, H.-C.; Goh, S.; Ban, H.; Kim, J. S.; Kim, J.-H.; Moon, J. Elucidation of the Formation Mechanism of Highly Oriented Multiphase Ruddlesden-Popper Perovskite Solar Cells. *ACS Energy Lett.* **2021**, *6*, 249–260.
- (17) Deng, Y.; Brackle, C. H. V.; Dai, X.; Zhao, J.; Chen, B.; Huang, J. Tailoring solvent coordination for high-speed, room-temperature blading of perovskite photovoltaic films. *Sci. Adv.* **2019**, *5*, No. eaax7537.
- (18) Cai, Y.; Cui, J.; Chen, M.; Zhang, M.; Han, Y.; Qian, F.; Zhao, H.; Yang, S.; Yang, Z.; Bian, H.; Wang, T.; Guo, K.; Cai, M.; Dai, S.; Liu, Z.; Liu, S. Multifunctional Enhancement for Highly Stable and Efficient Perovskite Solar Cells. *Adv. Funct. Mater.* **2021**, *31*, 2005776.
- (19) Kim, J. H.; Kim, Y. R.; Park, B.; Hong, S.; Hwang, I. W.; Kim, J.; Kwon, S.; Kim, G.; Kim, H.; Lee, K. Simultaneously Passivating Cation and Anion Defects in Metal Halide Perovskite Solar Cells Using a Zwitterionic Amino Acid Additive. *Small* **2021**, *17*, No. e2005608.
- (20) Ye, T.; Wang, X.; Wang, K.; Ma, S.; Yang, D.; Hou, Y.; Yoon, J.; Wang, K.; Priya, S. Localized Electron Density Engineering for Stabilized B- γ CsSnI₃-Based Perovskite Solar Cells with Efficiencies > 10%. *ACS Energy Lett.* **2021**, *6*, 1480–1489.
- (21) Chen, B.; Rudd, P. N.; Yang, S.; Yuan, Y.; Huang, J. Imperfections and their passivation in halide perovskite solar cells. *Chem. Soc. Rev.* **2019**, *48*, 3842–3867.
- (22) Chen, N.; Yi, X.; Zhuang, J.; Wei, Y.; Zhang, Y.; Wang, F.; Cao, S.; Li, C.; Wang, J. An Efficient Trap Passivator for Perovskite Solar Cells: Poly(propylene glycol) bis(2-aminopropyl ether). *Nano-Micro Lett.* **2020**, *12*, 177.
- (23) Zheng, X.; Hou, Y.; Bao, C.; Yin, J.; Yuan, F.; Huang, Z.; Song, K.; Liu, J.; Troughton, J.; Gasparini, N.; Zhou, C.; Lin, Y.; Xue, D.-J.; Chen, B.; Johnston, A. K.; Wei, N.; Hedhili, M. N.; Wei, M.; Alsalloum, A. Y.; Maity, P.; Turedi, B.; Yang, C.; Baran, D.; Anthopoulos, T. D.; Han, Y.; Lu, Z.-H.; Mohammed, O. F.; Gao, F.; Sargent, E. H.; Bakr, O. M. Managing grains and interfaces via ligand anchoring enables 22.3%-efficiency inverted perovskite solar cells. *Nat. Energy* **2020**, *5*, 131–140.
- (24) Wang, Q.; Zheng, X.; Deng, Y.; Zhao, J.; Chen, Z.; Huang, J. Stabilizing the α -Phase of CsPbI₃ Perovskite by Sulfobetaine Zwitterions in One-Step Spin-Coating Films. *Joule* **2017**, *1*, 371–382.
- (25) Zhou, Q.; Qiu, J.; Wang, Y.; Yu, M.; Liu, J.; Zhang, X. Multifunctional Chemical Bridge and Defect Passivation for Highly Efficient Inverted Perovskite Solar Cells. *ACS Energy Lett.* **2021**, *6*, 1596–1606.
- (26) Deng, Y.; Zheng, X.; Bai, Y.; Wang, Q.; Zhao, J.; Huang, J. Surfactant-controlled ink drying enables high-speed deposition of perovskite films for efficient photovoltaic modules. *Nat. Energy* **2018**, *3*, 560–566.
- (27) Wang, R.; Xue, J.; Wang, K.-L.; Wang, Z.-K.; Luo, Y.; Fenning, D.; Xu, G.; Nuryeva, S.; Huang, T.; Zhao, Y.; Yang, J. L.; Zhu, J.; Wang, M.; Tan, S.; Yavuz, I.; Houk, K. N.; Yang, Y. Constructive molecular configurations for surface-defect passivation of perovskite photovoltaics. *Science* **2019**, *366*, 1509–1513.
- (28) Wang, K.; Wu, C.; Hou, Y.; Yang, D.; Ye, T.; Yoon, J.; Sanghadasa, M.; Priya, S. Isothermally crystallized perovskites at room-temperature. *Energy Environ. Sci.* **2020**, *13*, 3412–3422.
- (29) Green, M.; Dunlop, E.; Hohl-Ebinger, J.; Yoshita, M.; Kopidakis, N.; Hao, X. Solar cell efficiency tables (version 57). *Prog. Photovoltaics* **2021**, *29*, 3–15.
- (30) Feng, W.; Zhang, C.; Zhong, J.-X.; Ding, L.; Wu, W.-Q. Correlated alkyl chain length with defect passivation efficacy in perovskite solar cells. *Chem. Commun.* **2020**, *56*, 5006–5009.
- (31) Duan, J.; Wang, Y.; Yang, X.; Tang, Q. Alkyl Chain Regulated Charge Transfer in Fluorescent Inorganic CsPbBr₃ Perovskite Solar Cells. *Angew. Chem., Int. Ed.* **2020**, *59*, 4391–4395.
- (32) Wu, G.; Yang, T.; Li, X.; Ahmad, N.; Zhang, X.; Yue, S.; Zhou, J.; Li, Y.; Wang, H.; Shi, X.; Liu, S.; Zhao, K.; Zhou, H.; Zhang, Y. Molecular Engineering for Two-Dimensional Perovskites with Photovoltaic Efficiency Exceeding 18%. *Matter* **2021**, *4*, 582–599.
- (33) Li, F.; Xie, Y.; Hu, Y.; Long, M.; Zhang, Y.; Xu, J.; Qin, M.; Lu, X.; Liu, M. Effects of Alkyl Chain Length on Crystal Growth and Oxidation Process of Two-Dimensional Tin Halide Perovskites. *ACS Energy Lett.* **2020**, *5*, 1422–1429.
- (34) Zhu, Z.; Chueh, C. C.; Li, N.; Mao, C.; Jen, A. K. Realizing Efficient Lead-Free Formamidinium Tin Triiodide Perovskite Solar Cells via a Sequential Deposition Route. *Adv. Mater.* **2018**, *30*, 1703800.
- (35) Xue, J.; Wang, R.; Wang, K. L.; Wang, Z. K.; Yavuz, I.; Wang, Y.; Yang, Y.; Gao, X.; Huang, T.; Nuryeva, S.; Lee, J. W.; Duan, Y.; Liao, L. S.; Kaner, R.; Yang, Y. Crystalline Liquid-like Behavior: Surface-Induced Secondary Grain Growth of Photovoltaic Perovskite Thin Film. *J. Am. Chem. Soc.* **2019**, *141*, 13948–13953.
- (36) Ma, Z.; Zhou, W.; Huang, D.; Liu, Q.; Xiao, Z.; Jiang, H.; Yang, Z.; Zhang, W.; Huang, Y. Nicotinamide as Additive for Microcrystalline and Defect Passivated Perovskite Solar Cells with 21.7% Efficiency. *ACS Appl. Mater. Interfaces* **2020**, *12*, 52500–52508.
- (37) Xu, W.; Hu, Q.; Bai, S.; Bao, C.; Miao, Y.; Yuan, Z.; Borzda, T.; Barker, A. J.; Tyukalova, E.; Hu, Z.; Kawecki, M.; Wang, H.; Yan, Z.; Liu, X.; Shi, X.; Uvdal, K.; Fahlman, M.; Zhang, W.; Duchamp, M.; Liu, J.-M.; Petrozza, A.; Wang, J.; Liu, L.-M.; Huang, W.; Gao, F. Rational molecular passivation for high-performance perovskite light-emitting diodes. *Nat. Photonics* **2019**, *13*, 418–424.
- (38) Wang, Y.; Yuan, J.; Zhang, X.; Ling, X.; Larson, B. W.; Zhao, Q.; Yang, Y.; Shi, Y.; Luther, J. M.; Ma, W. Surface Ligand

Management Aided by a Secondary Amine Enables Increased Synthesis Yield of CsPbI₃ Perovskite Quantum Dots and High Photovoltaic Performance. *Adv. Mater.* **2020**, *32*, 2000449.

(39) Shi, J.; Li, F.; Jin, Y.; Liu, C.; Cohen-Kleinstein, B.; Yuan, S.; Li, Y.; Wang, Z. K.; Yuan, J.; Ma, W. In Situ Ligand Bonding Management of CsPbI₃ Perovskite Quantum Dots Enables High-Performance Photovoltaics and Red Light-Emitting Diodes. *Angew. Chem., Int. Ed.* **2020**, *59*, 22230–22237.

(40) Zhang, L.; Zhang, Q.; Xing, X.; Jiang, Y.; He, T.; Huang, Y.; Ma, Z.; Yang, J.; Yuan, M. Conjugated Alkylamine by Two-Step Surface Ligand Engineering in CsPbBr₃ Perovskite Nanocrystals for Efficient Light-Emitting Diodes. *ChemNanoMat* **2019**, *5*, 318–322.

(41) Wu, W. Q.; Rudd, P. N.; Wang, Q.; Yang, Z.; Huang, J. Blading Phase-Pure Formamidinium-Alloyed Perovskites for High-Efficiency Solar Cells with Low Photovoltage Deficit and Improved Stability. *Adv. Mater.* **2020**, *32*, 2000995.

(42) Wang, F.; Geng, W.; Zhou, Y.; Fang, H. H.; Tong, C. J.; Loi, M. A.; Liu, L. M.; Zhao, N. Phenylalkylamine Passivation of Organolead Halide Perovskites Enabling High-Efficiency and Air-Stable Photovoltaic Cells. *Adv. Mater.* **2016**, *28*, 9986–9992.

(43) Kim, J.; Yun, A. J.; Gil, B.; Lee, Y.; Park, B. Triamine-Based Aromatic Cation as a Novel Stabilizer for Efficient Perovskite Solar Cells. *Adv. Funct. Mater.* **2019**, *29*, 1905190.

(44) Zhao, S.; Xie, J.; Cheng, G.; Xiang, Y.; Zhu, H.; Guo, W.; Wang, H.; Qin, M.; Lu, X.; Qu, J.; Wang, J.; Xu, J.; Yan, K. General Nondestructive Passivation by 4-Fluoroaniline for Perovskite Solar Cells with Improved Performance and Stability. *Small* **2018**, *14*, No. e1803350.

(45) Li, H.; Song, J.; Pan, W.; Xu, D.; Zhu, W. A.; Wei, H.; Yang, B. Sensitive and Stable 2D Perovskite Single-Crystal X-ray Detectors Enabled by a Supramolecular Anchor. *Adv. Mater.* **2020**, *32*, 2003790.

(46) Wan, F.; Ke, L.; Yuan, Y.; Ding, L. Passivation with crosslinkable diamine yields 0.1 V non-radiative V_{oc} loss in inverted perovskite solar cells. *Sci. Bull.* **2021**, *66*, 417–420.

(47) Wang, H.; Qin, Z.; Xie, J.; Zhao, S.; Liu, K.; Guo, X.; Li, G.; Lu, X.; Yan, K.; Xu, J. Efficient Slantwise Aligned Dion-Jacobson Phase Perovskite Solar Cells Based on Trans-1,4-Cyclohexanediamine. *Small* **2020**, *16*, No. e2003098. Jokar, E.; Cheng, P.-Y.; Lin, C.-Y.; Narra, S.; Shahbazi, S.; Wei-Guang Diao, E. Enhanced Performance and Stability of 3D/2D Tin Perovskite Solar Cells Fabricated with a Sequential Solution Deposition. *ACS Energy Lett.* **2021**, *6*, 485–492.

(48) Wang, Y.; Zhou, Y.; Zhang, T.; Ju, M.-G.; Zhang, L.; Kan, M.; Li, Y.; Zeng, X. C.; Padture, N. P.; Zhao, Y. Integration of Functionalized Graphene Nano-Network into Planar Perovskite Absorber for High Efficiency Large Area Solar Cells. *Mater. Horiz.* **2018**, *5*, 868–873.

(49) Kamarudin, M. A.; Hirotani, D.; Wang, Z.; Hamada, K.; Nishimura, K.; Shen, Q.; Toyoda, T.; Iikubo, S.; Minemoto, T.; Yoshino, K.; Hayase, S. Suppression of Charge Carrier Recombination in Lead-Free Tin Halide Perovskite via Lewis Base Post-treatment. *J. Phys. Chem. Lett.* **2019**, *10*, 5277–5283.

(50) Lv, Y.; Zhang, H.; Wang, J.; Chen, L.; Bian, L.; An, Z.; Qian, Z.; Ren, G.; Wu, J.; Nuesch, F.; Huang, W. All-in-One Deposition to Synergistically Manipulate Perovskite Growth for High-Performance Solar Cell. *Research* **2020**, *2020*, 2763409.

(51) Zhang, H.; Ren, X.; Chen, X.; Mao, J.; Cheng, J.; Zhao, Y.; Liu, Y.; Milic, J.; Yin, W.-J.; Grätzel, M.; Choy, W. C. H. Improving the stability and performance of perovskite solar cells via off-the-shelf post-device ligand treatment. *Energy Environ. Sci.* **2018**, *11*, 2253–2262.

(52) Li, T.; Wang, S.; Yang, J.; Pu, X.; Gao, B.; He, Z.; Cao, Q.; Han, J.; Li, X. Multiple functional groups synergistically improve the performance of inverted planar perovskite solar cells. *Nano Energy* **2021**, *82*, 105742.

(53) Xiong, S.; Hou, Z.; Zou, S.; Lu, X.; Yang, J.; Hao, T.; Zhou, Z.; Xu, J.; Zeng, Y.; Xiao, W.; Dong, W.; Li, D.; Wang, X.; Hu, Z.; Sun, L.; Wu, Y.; Liu, X.; Ding, L.; Sun, Z.; Fahlman, M.; Bao, Q. Direct Observation on p- to n-Type Transformation of Perovskite Surface

Region during Defect Passivation Driving High Photovoltaic Efficiency. *Joule* **2021**, *5*, 467–480.

(54) Yang, S.; Dai, J.; Yu, Z.; Shao, Y.; Zhou, Y.; Xiao, X.; Zeng, X. C.; Huang, J. Tailoring Passivation Molecular Structures for Extremely Small Open-Circuit Voltage Loss in Perovskite Solar Cells. *J. Am. Chem. Soc.* **2019**, *141*, 5781–5787.

(55) Zhao, Y.; Zhu, P.; Huang, S.; Tan, S.; Wang, M.; Wang, R.; Xue, J.; Han, T. H.; Lee, S. J.; Zhang, A.; Huang, T.; Cheng, P.; Meng, D.; Lee, J. W.; Marian, J.; Zhu, J.; Yang, Y. Molecular Interaction Regulates the Performance and Longevity of Defect Passivation for Metal Halide Perovskite Solar Cells. *J. Am. Chem. Soc.* **2020**, *142*, 20071–20079.

(56) Li, N.; Tao, S.; Chen, Y.; Niu, X.; Onwudinanti, C. K.; Hu, C.; Qiu, Z.; Xu, Z.; Zheng, G.; Wang, L.; Zhang, Y.; Li, L.; Liu, H.; Lun, Y.; Hong, J.; Wang, X.; Liu, Y.; Xie, H.; Gao, Y.; Bai, Y.; Yang, S.; Brocks, G.; Chen, Q.; Zhou, H. Cation and anion immobilization through chemical bonding enhancement with fluorides for stable halide perovskite solar cells. *Nat. Energy* **2019**, *4*, 408–415.

(57) Liu, K.; Liang, Q.; Qin, M.; Shen, D.; Yin, H.; Ren, Z.; Zhang, Y.; Zhang, H.; Fong, P. W. K.; Wu, Z.; Huang, J.; Hao, J.; Zheng, Z.; So, S. K.; Lee, C.-S.; Lu, X.; Li, G. Zwitterionic-Surfactant-Assisted Room-Temperature Coating of Efficient Perovskite Solar Cells. *Joule* **2020**, *4*, 2404–2425.

(58) He, J.; Liu, J.; Hou, Y.; Wang, Y.; Yang, S.; Yang, H. G. Surface chelation of cesium halide perovskite by dithiocarbamate for efficient and stable solar cells. *Nat. Commun.* **2020**, *11*, 4237.

(59) Chen, S.; Deng, Y.; Gu, H.; Xu, S.; Wang, S.; Yu, Z.; Blum, V.; Huang, J. Trapping lead in perovskite solar modules with abundant and low-cost cation-exchange resins. *Nat. Energy* **2020**, *5*, 1003–1011.